SYNTHESIS OF AMINE-FUNCTIONALIZED BIS(IMIDAZOLIUM)BORATE SALTS: NOVEL BIS(CARBENE)BORATE LIGAND PRECURSORS

by

AGELIKI KARAGIANNIS

A Dissertation submitted to the

Graduate School-Newark

Rutgers, The State University of New Jersey

in partial fulfillment of the requirements

for the degree of

Master of Science

Graduate Program in Chemistry

Written under the direction of

Professor Demyan Prokopchuk

and approved by

_____

_____

_____

Newark, New Jersey

May 2020

ABSTRACT OF THE DISSERTATION

Synthesis of Amine-functionalized Bis(imidazolium)borate Salts: Novel Bis(carbene)borate Ligand Precursors

By AGELIKI KARAGIANNIS

Dissertation Director:
Professor Demyan Prokopchuk

N-heterocyclic carbenes (NHCs), commonly derived from *N,N'*-disubstituted imidazolium salts, have gained popularity since their isolation by Arduengo in 1991 and their application as ligands for catalysis by Herrmann in the mid-1990s. An underexplored area of research is the examination of chelating ligands incorporating amine-functionalized bis(NHC) ligands. This thesis focuses on the synthesis of novel bis(imidazolium) borate salts and the preliminary formation of their NHCs. Early attempts of reacting imidazoles with chlorobis(amino)borane reagents yielded incomplete reactions or decomposition, which are likely the consequence of a steric and/or electronic mismatch between boron and its attached amines. After testing several chloroaminoborane reagents, two novel amine-functionalized bis(imidazolium)borate salts have been successfully synthesized and characterized. By reacting 1-*tert*-butylimidazole (^{tBu}Im) or 1-methylimidazole (^{Me}Im) with $^{i}Pr_2N(Ph)BCl$ at room temperature, the

salts **[^{i}Pr$_2$NB(Ph)(^{tBu}Im)$_2$][OTf]** and **[^{i}Pr$_2$NB(Ph)(^{Me}Im)$_2$][OTf]** (OTf = trifluroomethanesulfonate) can be prepared using a two-step, one-pot synthetic protocol. Halide abstraction using AgOTf to form the proposed intermediate **^{i}Pr$_2$NB(Ph)OTf**, followed by imidazole addition readily produces the target imidazolium borate salts. Optimization efforts resulted in the discovery of a solvent-dependent mechanism in CH_3CN versus CH_2Cl_2 during addition of AgOTf to $^{i}Pr_2NB(Ph)Cl$. In both solvents, the desired product is obtained, however the coordinating effects of CH_3CN may play a role in minimizing undesirable product formation. Overall, a reliable synthetic method to obtain amine-functionalized bis(imidazolium)borate salts is presented. Preliminary data suggests that deprotonation leads to carbene formation, however more experiments are needed to fully characterize the product. This work holds promise to prepare novel bis(carbene)aminoborates as proton-responsive ligands for electrocatalytic H_2 oxidation/production.

Acknowledgements

First and foremost, I would like to thank my research advisor, Dr. Demyan Prokopchuk, for giving me the opportunity to join his research group and for his invaluable guidance, motivation, and patience with my thesis project. I am sincerely grateful for all that I have learned since the beginning of this opportunity. I would also like to thank my fellow lab mates, Práxedes Sánchez, Bhumika Goel, Lirong Li, David Tresp, Meroline Bazile, and Christeen Shenoda for all their help and friendship. Lastly, this opportunity would not have been possible without my coworkers at LANXESS-Perth Amboy and their willingness to cover my shifts so that I could conduct my research during the day at Rutgers University.

Table of Contents

List of Schemes

List of Figures

Introduction

The ever-increasing energy consumption along with the environmental concerns surrounding the immense use of fossil fuels has initiated a global movement towards the discovery and invention of carbon-neutral alternatives for energy production. Renewable energy resources, such as solar and wind, have the potential to replace fossil fuels as our predominant energy sources, but efficient storage of their electrical energy is critically needed.[1-3] A promising approach is the conversion of this intermittently generated electrical energy into a fuel by forging new chemical bonds. Hydrogen is the simplest fuel and the most attractive energy carrier for a carbon-neutral future – it is a clean, inexhaustible, high-energy-content molecule that can be produced by the reduction of two protons with two electrons or cleaved by oxidation (eq 1).[4-6]

$$2H^+ + 2e^- \rightleftharpoons H_2 \qquad \textbf{(1)}$$

An eco-friendly method to produce hydrogen from renewable energy sources is by polymer electrolyte membrane (PEM) electrolysis, which consumes energy to split water into hydrogen and oxygen (Fig I-1a).[7-8] Additionally, the chemical energy stored in the H—H bond can be converted back into electricity and water by using a fuel cell (Fig I-1b).[3-5] Thus, the production and oxidation of H_2,

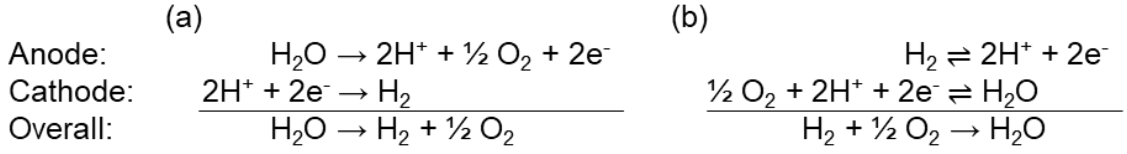

Fig I-1: The half-cell reactions in (a) PEM electrolysis and (b) fuel cells.

through utilization of both systems, allows this simple fuel to be stored and delivered in a carbon-neutral manner.

However, one major drawback in both PEM electrolysis and fuel cells is that the most effective catalyst for these systems is platinum, an expensive and low-abundance precious metal.[9] However, the discovery of nature's own energy-efficient hydrogenases[10] to produce and oxidize H_2 serves as a key inspirational model towards the synthesis of novel electrocatalysts using earth-abundant metals. Structural studies of the [FeFe]-hydrogenase cofactor show that the active site contains two iron atoms bridged by a di(thiomethyl)amine ligand, an $[Fe_4S_4]$ cluster, and CO/CN^- ligands bound to the iron centers (Fig I-2).[2,11] The position of

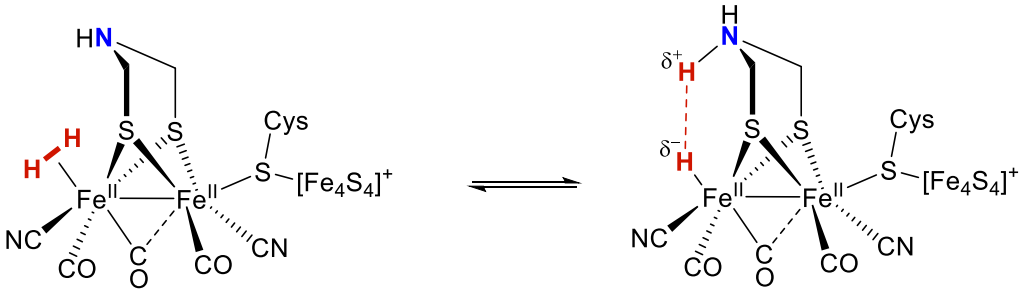

Fig I-2: Structural representation of the enzyme's active site and the pendant amine's role in the heterolytic cleavage/formation of the H—H bond (Cys = cysteine).

the amine base, pendant to the iron center, acts as a proton relay to facilitate the formation or heterolytic cleavage of the H—H bond, while the $[Fe_4S_4]$ cluster serves as an electron reservoir to transport electrons to and from the active site and the surrounding protein matrix.[12] The enzyme's ability to catalyze the production of H_2 from water with a turnover frequency as high as 9000 s^{-1} at 30 °C[13] has inspired

extensive research on the development of earth-abundant molecular electrocatalysts with comparable rates and efficiencies to replace platinum.

Dubois, Bullock, and coworkers have made great progress in the discovery and synthesis of efficient electrocatalysts for H_2 evolution and oxidation. Their research focuses on the synthesis of macrocyclic diphosphine ligands containing amine bases and their coordination to various earth-abundant metals. Nickel,[13-16] iron,[3] and cobalt[14,17-19] complexes that contain a $P^R{}_2N^{R'}{}_2$ (1,5-R'-3,7-R-1,5-diaza-3,7-diphosphacyclooctane) ligand have been successfully synthesized and characterized; a few are depicted in Fig I-3 along with their turnover frequencies (TOF) - the number of catalytic cycles per unit time – for the oxidation or production of H_2.

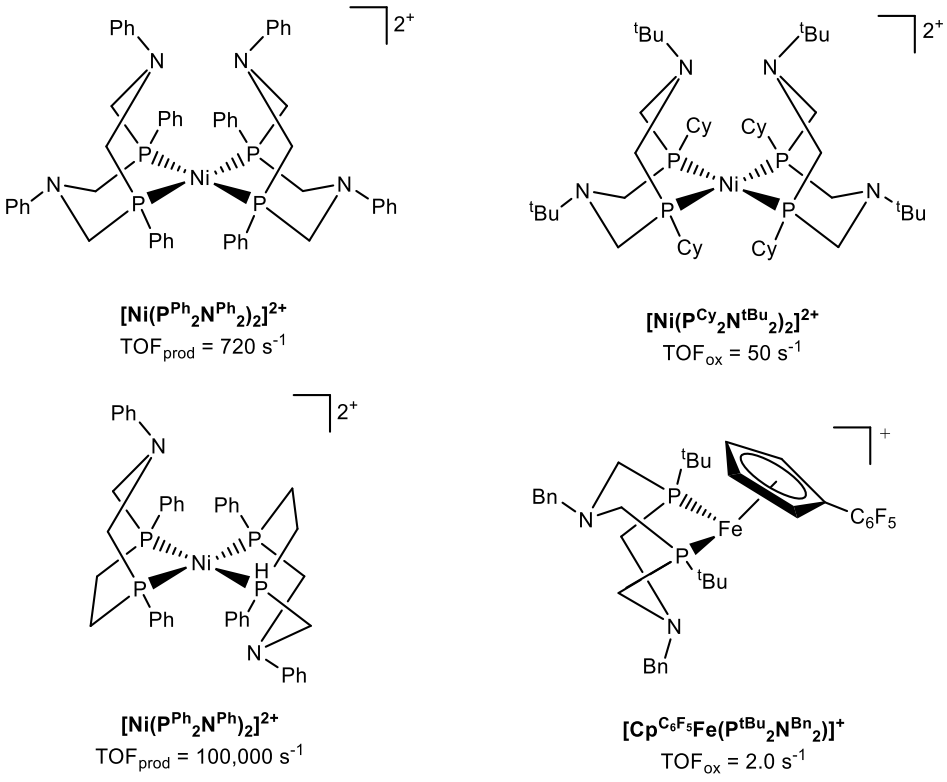

Fig I-3: Selected DuBois-Bullock H_2 production and oxidation catalysts.

Two valuable features the above complexes possess are their tunable steric and electronic properties. Substituent variations on the phosphorus and nitrogen atoms, located in the primary and secondary coordination spheres, respectively, force the catalyst to be biased towards either H_2 production or oxidation, as seen for the first row of complexes **[Ni(P$^{Ph}_2$N$^{Ph}_2$)$_2$]$^{2+}$** and **[Ni(P$^{Cy}_2$N$^{tBu}_2$)$_2$]$^{2+}$** in Fig I-3.[14-15] Additionally, modification of the diphosphine ligand to include only one amine base in its backbone enhances H_2 production, since it avoids formation of an intraligand NH···H bond that reduces catalytic activity (**[Ni(P$^{Ph}_2$N$^{Ph}_2$)$_2$]$^{2+}$** and **[Ni(P$^{Ph}_2$N^{Ph})$_2$]$^{2+}$**).[13-14] Furthermore, the choice of metal and ancillary ligands also influences whether one or two positioned amines are available for catalysis. Overall, these examples demonstrate why an understanding of the coordination spheres and a properly positioned pendant amine are fundamental in designing an efficient H_2 production or oxidation electrocatalyst that rivals the [FeFe]-hydrogenase cofactor.

Unfortunately, a disadvantage of DuBois-Bullock catalysts is their oxidation sensitive alkylphosphine functionalities, restricting their practical use.[20-21] However, N-heterocyclic carbenes (NHCs), which are also two electron L-type donor ligands, are generally less prone to oxidation or dissociation and may be better alternatives.[22-23] NHCs, which are a unique class of Fischer-type carbenes, are known to make strong σ-bonds to transition metals.[24-25] Density functional theory (DFT) calculation values indicate that the interaction energy (ΔE_{int}), a measure of metal-ligand bond stabilization energy, is between -52 and -58 kcal mol^{-1} for common monodentate NHCs while for $P(CH_3)_3$ it is between -41 and -46

kcal mol^{-1}.[26] This feature makes many catalysts that incorporate NHC-type ligands, instead of phosphines, more stable and potent two electron donors. This unique behavior is largely due to heteroatom stabilization, which promotes singlet carbene formation (Fig I-4, left). The lone pairs on nitrogen readily stabilize an empty p_π-

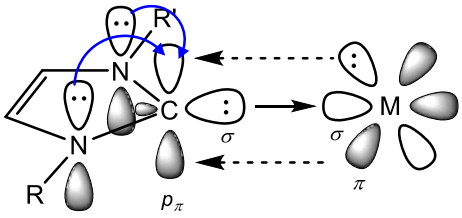

Fig I-4: Representation of the orbital interactions that influence the coordination of an NHC (left) with a transition metal.

orbital at the carbene carbon, forcing a singlet carbene configuration. Upon coordination to a metal, these paired carbene electrons donate into a vacant metal orbital of appropriate symmetry, thereby increasing electron density at the metal center. Weak π-backbonding from a metal π-type orbital to the NHC can occur, but σ-donation is predominant.[24-25] Collectively, these important features allow NHCs to act as potent electron donors. Furthermore, like phosphine ligands, NHCs are sterically and electronically tunable by altering the “wingtip" R substituents and heterocycle backbone.

Consequently, the search continues for novel molecular electrocatalysts that will rival platinum’s electrochemical catalytic performance[9] and efficiently link renewable and chemical energy to help create a carbon-neutral energy landscape. Aiming to study new ligand designs that may result in an improved electrocatalyst,

this Masters thesis focuses on the synthesis of amine-functionalized bis(imidazolium) borate salts, which are precursors to NHC ligands that contain a pendant amine. Inclusion of such functionalities would dramatically influence the primary and secondary coordination spheres and might enhance the stability and robustness of metal complexes, due to the powerful σ-donor properties of NHCs. Fig I-5 depicts the $P^{R}_{2}N^{R'}_{2}$ DuBois-Bullock ligand and the analogous proposed amine-functionalized bis(carbene)borate ligand.

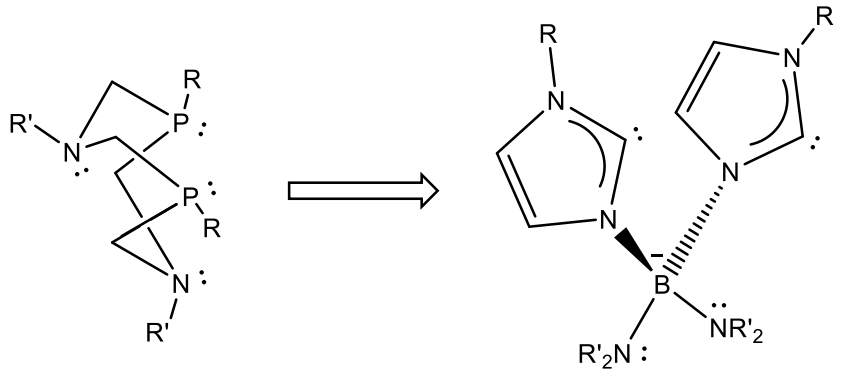

Fig I-5: Proposed ligand design, where R and R' are alkyl/aryl groups.

As illustrated by the DuBois-Bullock catalysts and the [FeFe]-hydrogenase cofactor, the key component for effective proton transfer is the presence of a pendant amine during catalysis. In the anticipated ligand, the amine-borane moiety would be in the secondary coordination sphere, where its expected structural orientation would position the nitrogen atom pendant to the metal center. In the presence of H_2, the amine base would promote the heterolytic cleavage of the H—H bond, as portrayed in Scheme I-1. The incorporation of the amine-borane would be essential to improve the electrocatalytic rate of the complex by assisting with

the intra- and intermolecular proton transfers required for proton reduction or the oxidation of H_2.

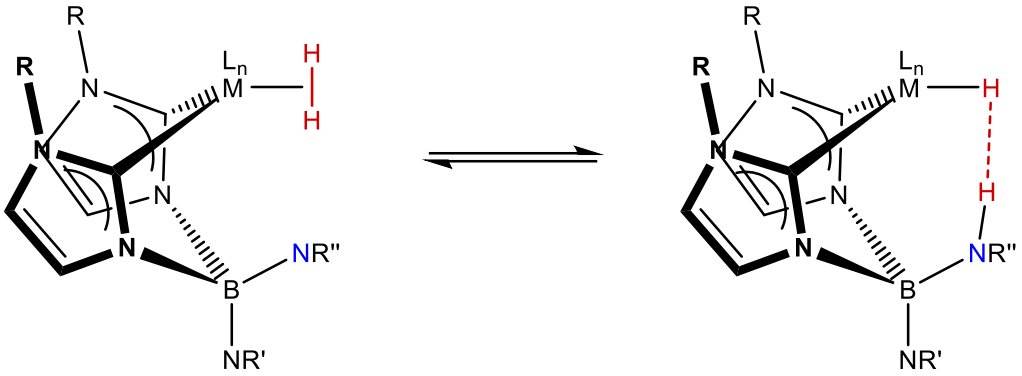

Scheme I-1: Anticipated ligand binding and heterolytic cleavage of H_2 by a metal complex.

Chapter 1 focuses on the various approaches examined to ultimately synthesize two novel amine-functionalized bis(imidazolium) borate salts. A solvent dependence on the reaction outcome was discovered, with weakly coordinating solvents such as CH_3CN appearing to be most suitable. Further research is currently under way to broaden the synthetic scope and synthesize the free carbene ligand, while future work will focus on the synthesis of transition metal complexes and their reactivity with H_2, protons, and electrons.

References

1. Lewis, N.S., Nocera, D.G., *PNAS* **2006**, *103*, 15729 – 15735
2. Bullock, R.M., Catalysis Without Precious Metals, **2010**, 1st ed. Wiley-VCH
3. Bullock, R.M., Helm, M.L., *Acc. Chem. Res.* **2015**, *48*, 2017 – 2026
4. Navarro, R.M., Peña, M.A., Fierro, J.L.G., *Chem. Rev.* **2007**, *107*, 3952 – 3991
5. Raugei, S., Helm, M.L., Hammes-Schiffer, S., Appel, A.M., O'Hagan, M., Wiedner, E.S., Bullock, R.M., *Inorg. Chem.* **2016**, *55*, 445 – 460
6. Shaw, W.J, Helm, M.L., Dubois, D.L., *Biochimica et Biophysica Acta*, **2013**, *1827*, 1123 – 1139
7. McKone, J.R., Marinescu, S.C., Brunschwig, B.S., Winkler, J.R., Gray, H.B., *Chem. Sci.* **2014**, *5*, 865 – 878
8. Kumar, S.S., Himabindu, V., *Materials Science for Energy Technologies* **2019**, *2*, 442 – 454
9. Lipman, T.E., Weber, A.Z., Fuel Cells and Hydrogen Production, **2019**, 2nd ed. Springer
10. Schilter, D., Camara, J.M., Huynh, M. T., Hammes-Schiffer, S., Rauchfuss, T.B., *Chem. Rev.* **2016**, *116*, 8693 – 8749
11. Artz, J.H., Zadvornyy, O.A., Mulder, D.W., Keable, S.M., Cohen, A.E., Ratzloff, M.W., Williams, S.G., Ginovska, B., Kumar, N., Song, J., McPhillips, S.E., Davidson, C.M., Lyubimov, A.Y., Pence, N., Schut, G.J., Jones, A.K., Soltis, S.M., Adams, M.W.W., Raugei, S., King, P.W., Peters, J.W., *J. Am. Chem. Soc.* **2020**, *142*, 1227 – 1235

12. Lubitz, W., Ogata, H., Rüdiger, O., Reijerse, E., *Chem. Rev.* **2014**, *114*, 4081 – 4148

13. Helm, M.L., Stewart, M.P., Bullock, R.M., DuBois, M.R., DuBois, D.L., *Science*, **2011**, *333*, 863 – 865

14. DuBois, D.L., *Inorg. Chem.* **2014**, *53*, 3935 – 3960

15. Wilson, A.D., Shoemaker, R.K., Miedaner, A., Muckerman, J.T., DuBois, D.L., DuBois, M.R., *PNAS*, **2007**, *104*, 6951 – 6956

16. Wilson, A.D., Newell, R.H., McNevin, M.J., Muckerman, J.T., DuBois, M.R., DuBois, D.L., *J. Am. Chem. Soc.* **2006**, *128*, 358 – 366

17. Yang, J.Y., Bullock, R.M, Shaw, W.J., Twamley, B., *J. Am. Chem. Soc.* **2009**, *131*, 5935 – 5945

18. Jacobsen, G.M., Yang, J.Y., Twamley, B., Wilson, A.D., Bullock, R.M., DuBois, M.R., DuBois, D.L., *Energy Environ. Sci.* **2008**, *1*, 167 – 174

19. DuBois, M.R, DuBois, D.L., *Acc. Chem. Res.* **2009**, *42*, 1974 – 1982

20. Buckler, S.A., *J. Am. Chem. Soc.* **1962**, *84*, 3093 – 3097

21. Grushin, V.V., *Chem. Rev.* **2004**, *104*, 1629 – 1662

22. Crabtree, R.H., The Organometallic Chemistry of the Transition Metals, **2009**, 5th ed. John Wiley & Sons, Inc.

23. Jacobsen, H., Correa, A., Poater, A., Costabile, C, Cavallo, L., *Coord. Chem. Rev.* **2009**, *253*, 687 – 703

24. Huynh, H.V., *Chem Rev.* **2018**, *118*, 9457 – 9492

25. Bourissou, D., Guerret, O., Gabbaï, F.P., Bertrand, G., *Chem Rev.* **2000**, *100*, 39 – 91

26. Tonner, R., Heydenrych, G., Frenking, G., *Chem. Asian. J.* **2007**, *2*, 1555 – 1567

Chapter 1

Synthesis of Amine-functionalized Bis(imidazolium) Borate Salts

1.1 Attempted Synthesis of $[(Me_2N)_2B(^{tBu}Im)_2][X]$

The core structure of the amine-functionalized bis(imidazolium) borate salt was inspired by an article published by Hofmann and coworkers.[1] The borate-bridged bis(imidazolium) salts $[R_2B(^{tBu}Im)_2][PF_6]$ (R = Ph or Me) were synthesized by utilizing the procedure depicted in the top of Scheme 1-1. The addition of

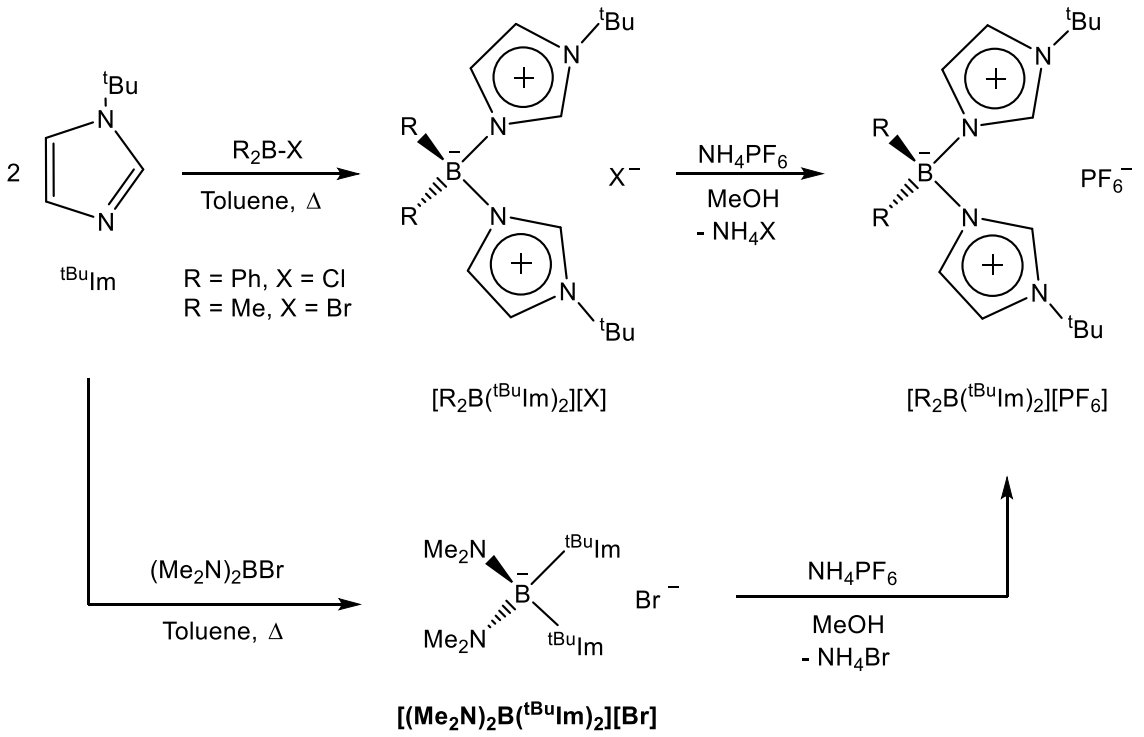

Scheme 1-1: Hoffman's synthetic approach for anionic ligands $[R_2B(^{tBu}Im)_2]$.

1-*tert*-butylimidazole (^{tBu}Im) to dialkyl- and diarylboron halides at room temperature, followed by reflux, afforded $[R_2B(^{tBu}Im)_2][X]$, where R = Ph, Me and X = Br, Cl. Subsequent treatment with ammonium hexafluorophosphate (NH_4PF_6)

in methanol yielded $[R_2B(^{tBu}Im)_2][PF_6]$. To incorporate the pendant amines (R = Me_2N) into a new imidazolium salt, **$[(Me_2N)_2B(^{tBu}Im)_2][Br]$**, commercially available $(Me_2N)_2BBr$ was reacted with two equivalents of ^{tBu}Im in a similar manner (Scheme 1-1, bottom). Following Hofmann's method to synthesize $[R_2B(^{tBu}Im)_2][X]$, a brown sticky solid was obtained. Integrations in the ^1H NMR spectrum indicated the presence of only one Me_2N group bonded to boron, suggesting that amine dissociation is taking place. Additional experiments were conducted, which varied the addition rate and temperature, reflux temperature, and reaction solvent, however all ^1H NMR spectra indicated the presence of only one Me_2N group attached to boron. As shown in Scheme 1-1, anion metathesis was also attempted with NH_4PF_6 and KPF_6. The cleanest ^1H NMR spectrum (Fig 1-1) was obtained after an anion metathesis with NH_4PF_6 of an experiment in which the two reagents were added at -20 °C and stirred at room temperature for 24 hours.

The proposed product, **$[(Me_2N)B(X)(^{tBu}Im)_2][PF_6]$**, where **X** is likely OH^-, is depicted in Fig 1-1. The signal at 2.55 ppm indicates that the target molecule, **$[(Me_2N)_2B(^{tBu}Im)_2][PF_6]$**, was not synthesized: only six of the expected twelve H atoms are present. The proposed product likely has a hydroxyl group bonded to the boron atom because the ^{tBu}Im used was not rigorously dried with molecular sieves after vacuum distillation. In the presence of water or moisture, the starting reagent, $(Me_2N)_2BBr$, or its intermediate may be forming a strong B—OH bond and causing the dissociation of the one amine group.

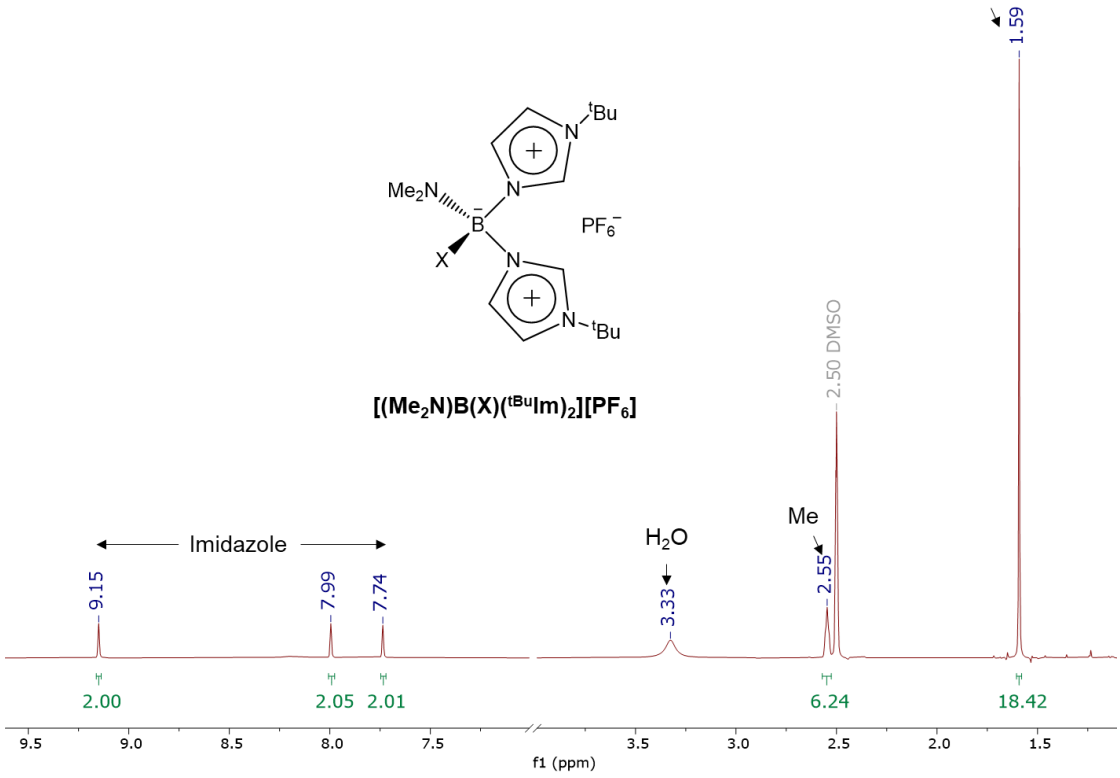

Fig 1-1: The ^{1}H NMR spectrum (500 MHz, DMSO-*d*$_6$) of the proposed product **[(Me$_2$N)B(X)(**^{tBu}**Im)$_2$][PF$_6$]** where **X** is likely OH^-.

Although the exact mechanism for B—N bond cleavage is unclear, a single crystal was obtained from the above experiment. A connectivity-only molecular structure of **[Me$_2$NH$_2$][Br]** was obtained (Fig 1-2) from the vapor diffusion of acetonitrile (MeCN) into diethyl ether inside an argon-filled glovebox, which further

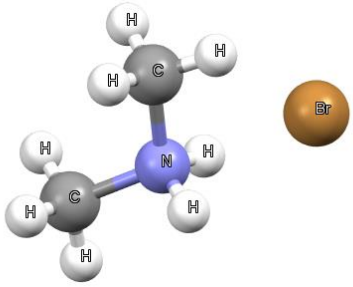

Fig 1-2: Molecular structure of **[Me$_2$NH$_2$][Br]** (connectivity only).

demonstrates the moisture sensitivity of the reagents involved. Thus, in the presence of excess water and prior to salt metathesis, $(Me_2N)_2BBr$ might react with water and ^{tBu}Im as shown in eq 2:

$$(Me_2N)_2BBr + 2\ ^{tBu}Im + 2\ H_2O \rightarrow \mathbf{[Me_2NH_2][Br]} + [Me_2NB(OH)(^{tBu}Im)_2][OH] \quad \mathbf{(2)}$$

However, even using rigorously dried solvents and reagents, reactions to synthesize **$[(Me_2N)_2B(^{tBu}Im)_2][PF_6]$** were unsuccessful. This may be due to B—N bond weakening from competing B—N π-bonding interactions through the lone pairs of both Me_2N groups, which are both sterically unencumbered. This perturbation may promote amine dissociation in the presence of a proton and/or hydroxide source, even in trace amounts. B—N bond cleavage has been observed in a similar case for the reaction of azole heterocycles with $B(NMe_2)_3$.[2]

1.2 Attempted Synthesis of $[(^iPr_2N)_2B(^{tBu}Im)_2][X]$

Since attempts with the amine reagent $(Me_2N)_2BBr$ did not yield the desired **$[(Me_2N)_2B(^{tBu}Im)_2][PF_6]$** salt, the sterically bulkier, electron rich amine $(^iPr_2N)_2BCl$ was synthesized using known literature protocols,[3] which might inhibit B—N bond cleavage. Following a modified version of the approach outlined in Scheme 1-1, the starting reagents ^{tBu}Im and $(^iPr_2N)_2BCl$ were added at -78 °C and stirred for 24 hours at room temperature (Scheme 1-2). The ^1H NMR spectrum of the resulting oily yellow-orange residue indicated an incomplete reaction (Fig 1-3**,** green) due to the presence of free ^{tBu}Im at 1.52 ppm. Refluxing the mixture in toluene did not decrease the amount of free ^{tBu}Im when compared to the monosubstituted

intermediate **($^{i}Pr_2N)_2B(^{tBu}Im)Cl,** whose *tert*-butyl resonance can be found at around 1.66 ppm (Fig 1-3, blue & purple). In all cases, the desired compound

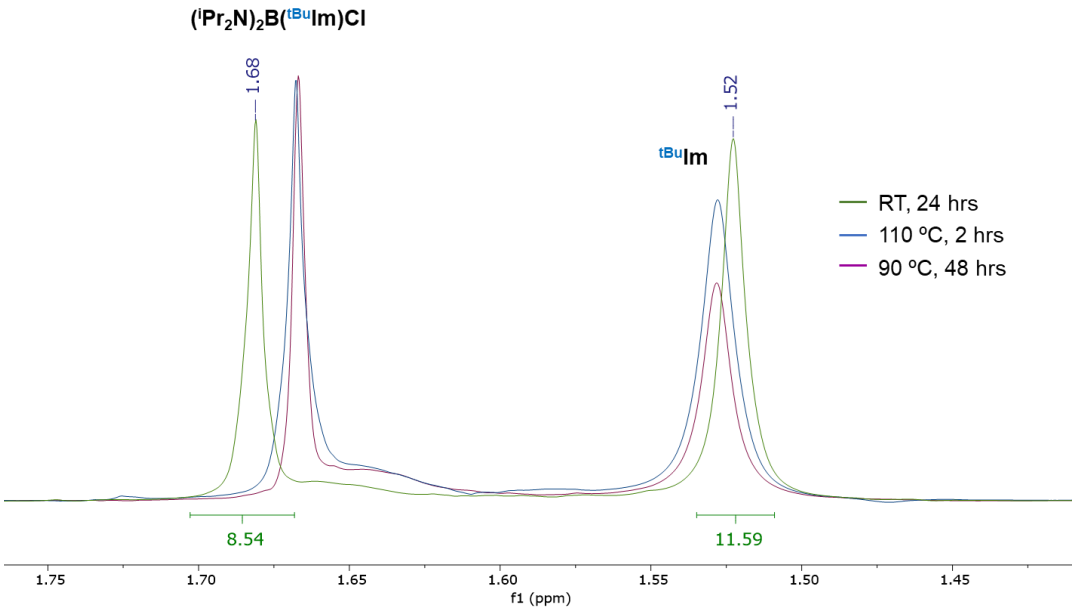

Fig 1-3: The aliphatic region from the ^{1}H NMR spectrum (500 MHz, CD_3CN) of the reaction of $(^{i}Pr_2N)_2BCl$ with 2 equiv. ^{tBu}Im under various reaction conditions.

$[(^{i}Pr_2N)_2B(^{tBu}Im)_2][Cl]$ did not form and large amounts of free imidazole were detected in all crude reaction mixtures. Furthermore, it is unclear what caused a chemical shift change in the NMR spectra after the reaction was refluxed. Thus, replacing the amine reagent $(Me_2N)_2BBr$ with $(^{i}Pr_2N)_2BCl$ inhibits B–N bond cleavage but instead prevents the coordination of two equivalents of ^{tBu}Im (Scheme 1-2).

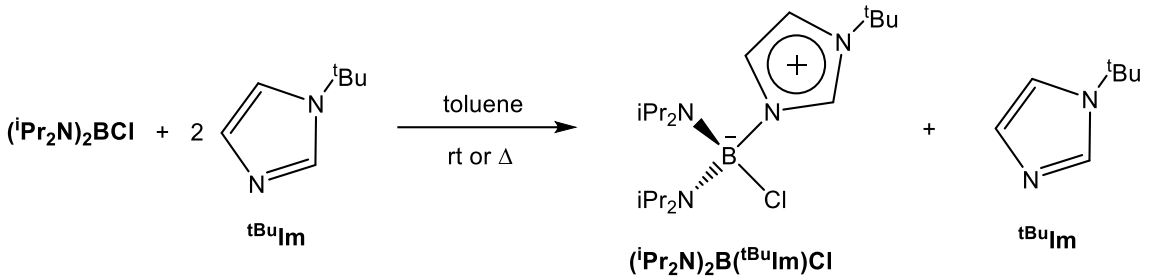

Scheme 1-2: Modified synthetic approach to react $(^{i}Pr_2N)_2BCl$ and ^{tBu}Im, producing **$(^{i}Pr_2N)_2B(^{tBu}Im)Cl$**.

Since direct addition of ^{tBu}Im with either $(Me_2N)_2BBr$ or $(^{i}Pr_2N)_2BCl$ failed to produce the desired imidazolium salts, multiple synthetic approaches were attempted, inspired by a report published by Smith and coworkers.[4] Their work describes a very similar dilemma and discovered that the introduction of a better leaving group on boron was successful for installing three alkylimidazoles at boron. In their case, exchanging the B-Cl bond of $PhBCl_2$ with a trifluoromethanesulfonate (OTf^-) anion (via Me_3SiOTf or AgOTf) or with B-I (via NaI) facilitated nucleophilic substitution with 3 equiv. ^{tBu}Im to yield tris(imidazolium)borate salts $[PhB(^{tBu}Im)_3][X]_2$. Scheme 1-3 depicts Methods **A**, **B**, and **C** utilized by Smith and coworkers, with modified stoichiometric ratios for the synthesis of the desired amine-functionalized bis(imidazolium) borate salts for this thesis project.

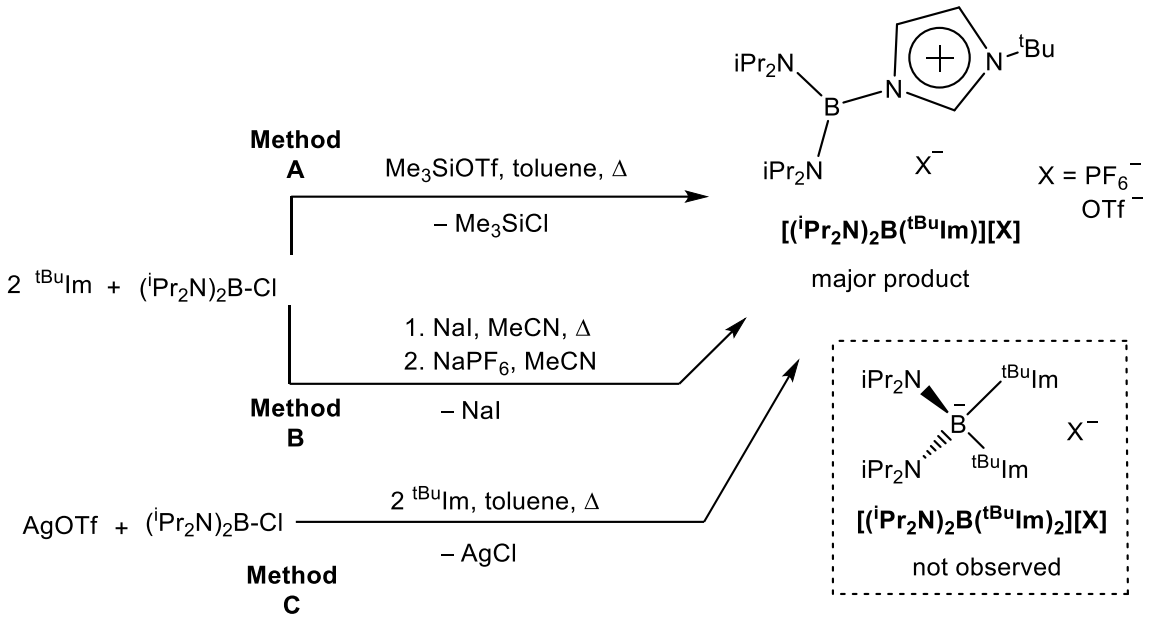

Scheme 1-3: Modification of Smith's methods[4] for the synthesis of the desired **[(^{i}Pr$_2$N)$_2$B(^{tBu}Im)$_2$][X]** salts.

Multiple attempts to synthesize compound **[(^{i}Pr$_2$N)$_2$B(^{tBu}Im)$_2$][OTf]** following Method **A** proved ineffective (Scheme 1-3, top). Increasing the temperature, time, and quantity of ^{tBu}Im showed no significant differences in all ^{1}H NMR spectra. In all cases, the proposed monosubstituted imidazolium borate salt forms, **[(^{i}Pr$_2$N)$_2$B(^{tBu}Im)][OTf]**, based on the integrations of the aliphatic and aromatic protons in the NMR spectra (Fig 1-4). Presumably, this is an intermediate that forms prior to nucleophilic attack of a second imidazole at boron to form the desired product. Fig 1-4 shows the three magnetically inequivalent imidazolium C–H protons at 9.14, 7.57, and 7.21 ppm. Furthermore, major signals also appeared at 8.58, 7.38, and 7.36 ppm, which were initially dismissed as impurities and/or reaction byproducts. However, these signals could also be evidence for self-assembled dimers or clusters of **[(^{i}Pr$_2$N)$_2$B(^{tBu}Im)][OTf]** in solution. A recent

series of articles on the solution state structures of imidazolium-based ionic liquids reports solvent- and anion-dependent chemical shift behavior, which is attributed to hydrogen bonding and aggregation between cations, anions, and solvent.[5-8] Additionally, the relative strength of hydrogen bonds between different molecules in solution have been qualitatively studied using diffusion-ordered NMR spectroscopy (DOSY).[9,10] These studies demonstrate how solvent choice influences hydrogen bonding by comparing their diffusion coefficients. Thus, the presence of the amines and triflate anions behaving as hydrogen bond acceptors with the imidazolium ring protons of **[(^{i}Pr$_2$N)$_2$B(^{tBu}Im)][OTf]** in solution may be promoting such behavior, based on the anion exchange reactions described below.

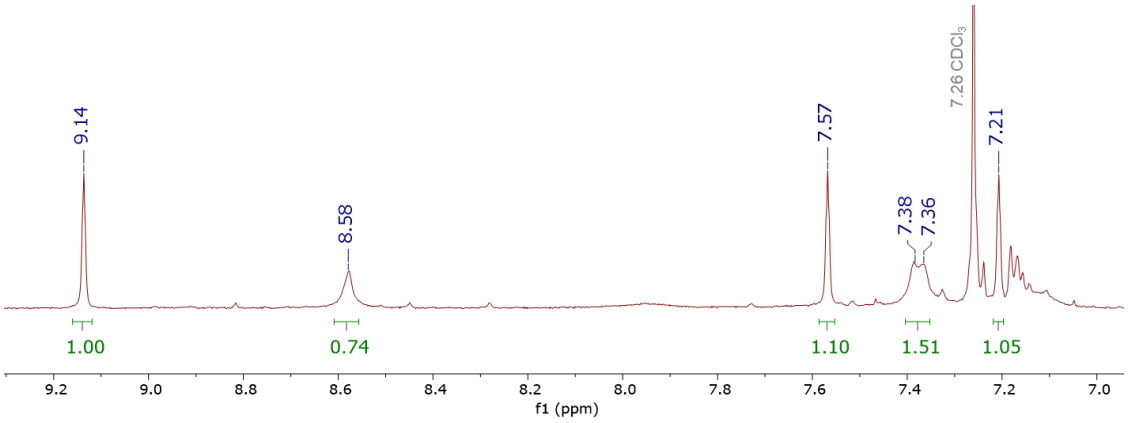

Fig 1-4: ^{1}H NMR spectrum (500 MHz, $CDCl_3$) of the aromatic region of **[(^{i}Pr$_2$N)$_2$B(^{tBu}Im)][OTf]** obtained by Method **A**.

Even though Methods **B** and **C** proved no more effective than Method **A** at producing the desired product, they help support the counter-anion effect described above. Using Method **B** produced cleaner spectra, which uses $NaPF_6$

to remove OTf, presumably forming **[(^{i}Pr$_2$N)$_2$B(^{tBu}Im)][PF$_6$]** and therefore minimal H-bonding and/or aggregation in solution. Unlike the OTf^- anion, PF_6^- discourages cation-anion hydrogen bonding interactions in solution due to its more diffuse anionic charge distribution. In particular, performing Method **C** followed by anion exchange of the OTf^- anion with KPF_6 immediately after heating to 110 °C, but prior to filtration, led to the cleanest ^{1}H NMR spectrum (Fig 1-5). Although minor signals still persist, aggregation and/or H-bonding is severely reduced.

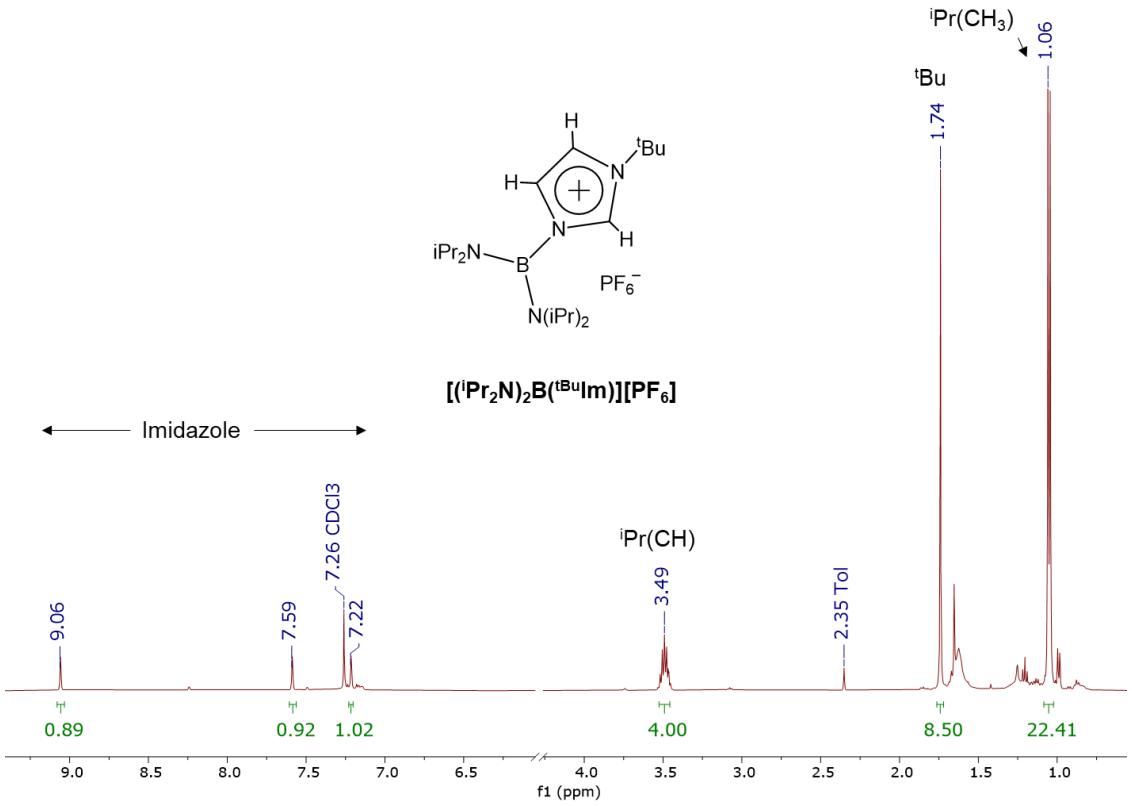

Fig 1-5: ^{1}H NMR spectrum (500 MHz, $CDCl_3$) of **[(^{i}Pr$_2$N)$_2$B(^{tBu}Im)][OTf]** obtained by Method **C**.

Nonetheless, all three methods failed to synthesize the target bis(imidazolium) borate salt, even with a large excess of ^{tBu}Im or by prolonged

heating (Scheme 1-3). The repeated formation of only the monosubstituted adduct implies that the presence of two $^{i}Pr_2N$ groups bonded to the boron atom may impose electronic and steric constraints towards nucleophilic addition of another equivalent of ^{tBu}Im (Fig 1-6). Although B–N bond dissociation does not occur, the lone pairs at $^{i}Pr_2N$ better stabilize boron's vacant p_{π}-orbital, making it a much weaker electrophile.

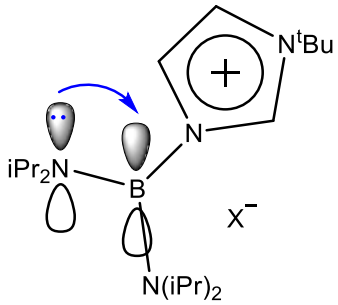

Fig 1-6: Representation of the orbital interactions that can weaken boron's electrophilicity, where X = Cl, OTf, or PF_6. The second $^{i}Pr_2N$ group's orbital contribution is not shown for clarity.

1.3 Synthesis of [^{i}Pr$_2$NB(Ph)(^{tBu}Im)$_2$][OTf] and [^{i}Pr$_2$NB(Ph)(^{Me}Im)$_2$][OTf]

To investigate the electronic and steric effects imposed by the reaction of precursors $(Me_2N)_2BBr$ and $(^{i}Pr_2N)_2BCl$ with ^{tBu}Im, a precursor that incorporates only one amine moiety bonded to boron was synthesized, $^{i}Pr_2NB(Ph)Cl$, using a modified synthetic protocol from the literature.[11] Following the modified version of Method **C** from Scheme 1-2, AgOTf was added to a solution of $^{i}Pr_2NB(Ph)Cl$ in toluene and stirred (Scheme 1-4, top). Next, two equivalents of ^{tBu}Im were added

and the solution was heated to 100 °C for 24 hours, followed by the addition of excess KPF_6 in THF and subsequent reaction workup. Surprisingly, these conditions led to loss of the amine substituent and produced the known tris(imidazolium)borane dication $[PhB(^{tBu}Im)_3][PF_6]_2$ as the major product.[4]

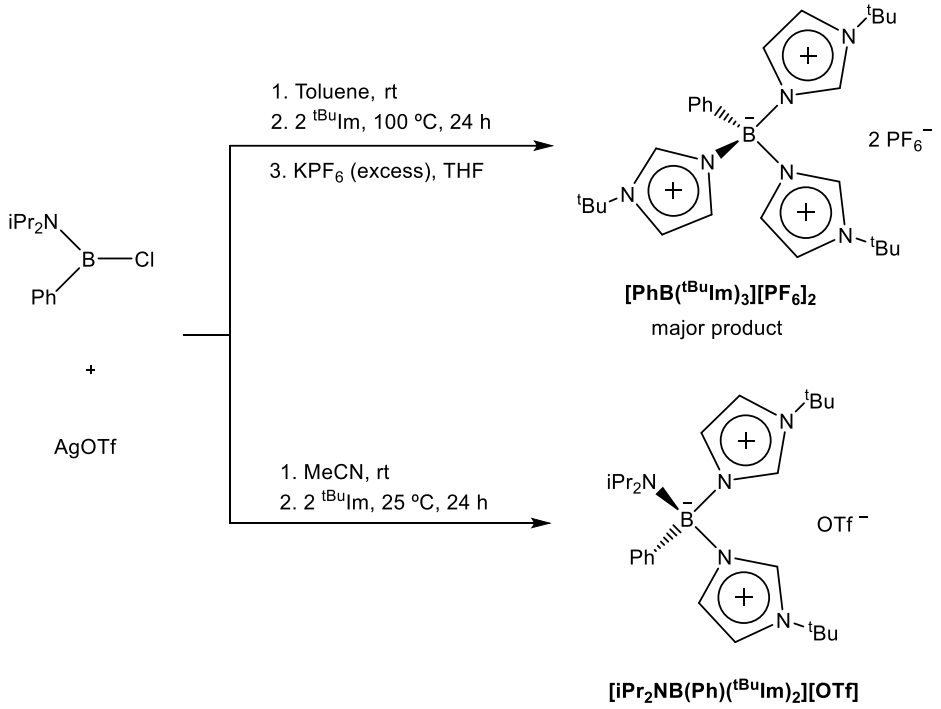

Scheme 1-4: Conditions used for the synthesis of the **$[PhB(^{tBu}Im)_3][PF_6]_2$** (major product) and **$[^{i}Pr_2NB(Ph)(^{tBu}Im)_2][OTf]$** salts (rt = room temperature).

The above reaction was repeated in acetonitrile at 70 °C. The crude ^1H NMR spectrum indicated that a mixture of tri-, di-, and mono-substituted imidazolium borate salts had formed. This observation suggests that the trisubstituted imidazolium salt is the thermodynamic product, while the desired disubstituted imidazolium salt is a kinetic product. To test this hypothesis, two solutions of AgOTf and $^{i}Pr_2NB(Ph)Cl$ were stirred for 20 min at room temperature, filtered, and then

two equivalents of ^{tBu}Im were added. Next, two J. Young tubes were prepared, where one was heated to 35 °C and the other was stirred at room temperature for 24 hours. Analysis by ^{1}H NMR showed that the room temperature reaction was much cleaner (Fig 1-7)**,** indicating that the desired amine-functionalized bis(imidazolium) borate salt **[^{i}Pr$_2$NB(Ph)(^{tBu}Im)$_2$][OTf]** was finally synthesized (Scheme 1-4, bottom).

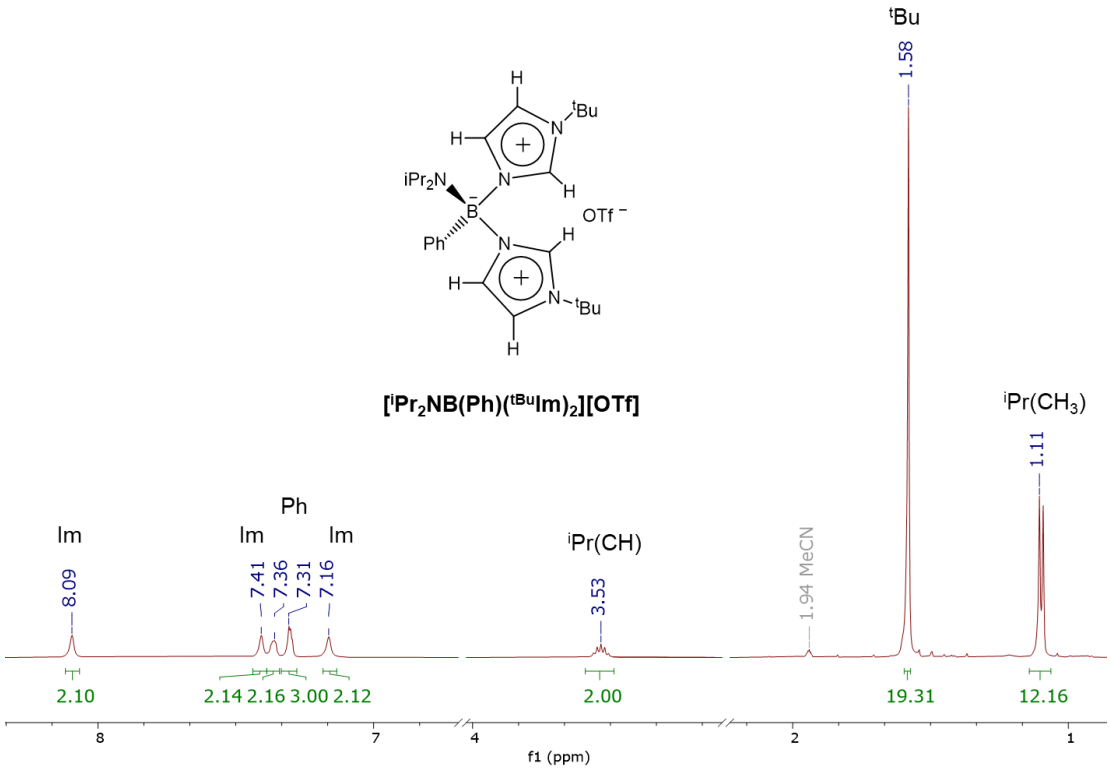

Fig 1-7: ^{1}H NMR spectrum (500 MHz, CD_3CN) of **[^{i}Pr$_2$NB(Ph)(^{tBu}Im)$_2$][OTf]**.

The reaction was repeated on a larger scale, washed with diethyl ether and pentane, and then dried to give a yellow-white powder in 46% isolated yield. Its analysis by ^{1}H NMR corresponds to the structure drawn in Fig 1-7; a noteworthy observation is that the spectrum shows minimal or no aggregation/H-bonding behavior under these reaction conditions, which might be the result of having one

less amine, using a more polar NMR solvent,[9,10] or both. Furthermore, ^{11}B, ^{19}F, ^{13}C, ^{1}H-^{13}C HSQC, and ^{1}H-^{13}C HMBC NMR all indicate that **[$^{i}Pr_2$NB(Ph)(^{tBu}Im)$_2$][OTf]** was successfully prepared. Fig 1-8 shows the ^{13}C NMR spectrum of **[$^{i}Pr_2$NB(Ph)(^{tBu}Im)$_2$][OTf]**, where the groups bonded to the boron center are color-coded to assist in their identification. The carbons of the imidazolium ring are at 135.87, 129.21, and 119.45 ppm and compare well with the known compound [$Ph_2B(^{tBu}Im)_2$][PF_6], where δ = 135.7, 125.1, and 119.9 ppm.[1]

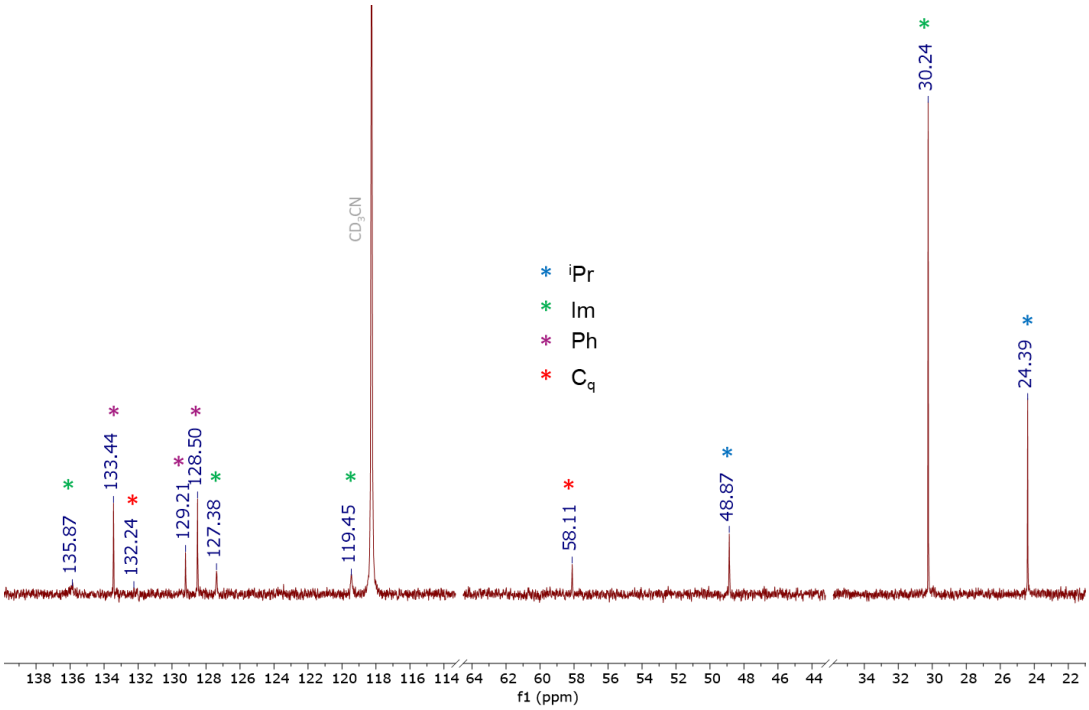

Fig 1-8: ^{13}C NMR spectrum (126 MHz, CD_3CN) of **[$^{i}Pr_2$NB(Ph)(^{tBu}Im)$_2$][OTf]**.

The successful synthesis of **[$^{i}Pr_2$NB(Ph)(^{tBu}Im)$_2$][OTf]** inspired the synthesis of the methylimidazole derivative, **[$^{i}Pr_2$NB(Ph)(^{Me}Im)$_2$][OTf]**, where 1-methylimidazole is used (Scheme 1-5). Following an identical procedure as for **[$^{i}Pr_2$NB(Ph)(^{tBu}Im)$_2$][OTf]**, the compound **[$^{i}Pr_2$NB(Ph)(^{Me}Im)$_2$][OTf]** was easily prepared with a 92% isolated yield.

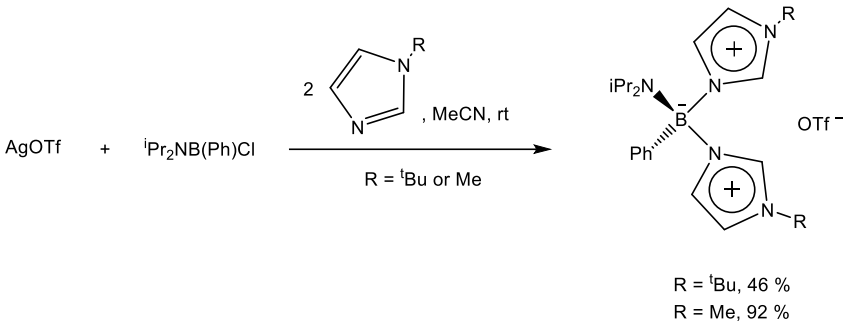

Scheme 1-5: General synthetic protocol of **[^{i}Pr$_2$NB(Ph)(^{tBu}Im)$_2$][OTf]** and **[^{i}Pr$_2$NB(Ph)(^{Me}Im)$_2$][OTf]** (rt = room temperature).

Analysis and characterization using ^{1}H, ^{11}B, ^{19}F, ^{13}C, ^{1}H-^{13}C HSQC, and ^{1}H-^{13}C HMBC NMR indicate that **[^{i}Pr$_2$NB(Ph)(^{Me}Im)$_2$][OTf]** was synthesized. Figs 1-9 and 1-10 show the ^{1}H and ^{13}C NMR spectra, respectively. After multiple attempts using different solvent combinations, growing single crystals suitable for X-ray diffraction has been unsuccessful to date for both imidazolium salts.

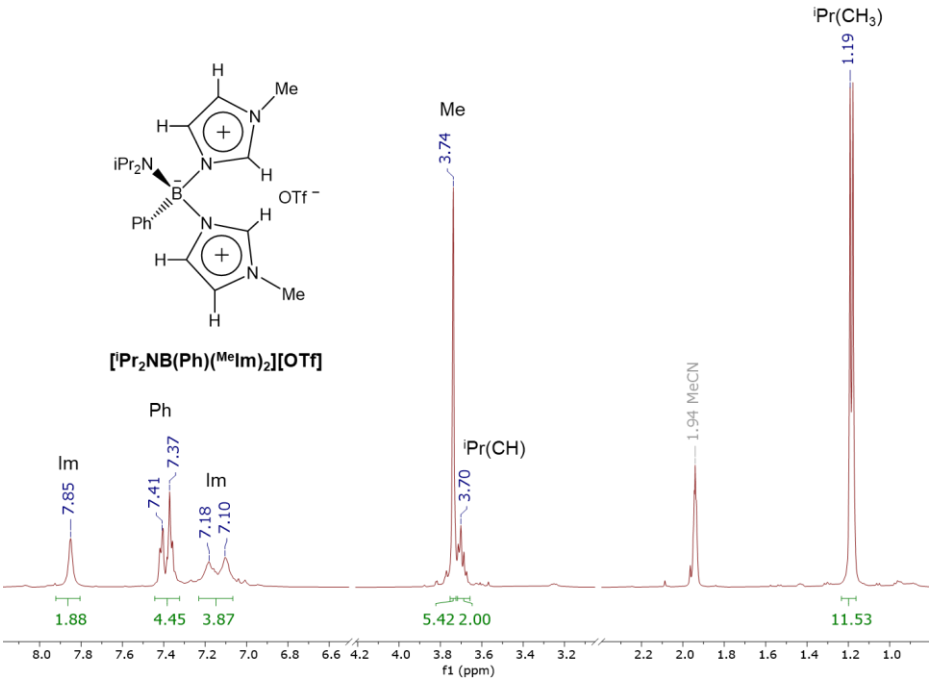

Fig 1-9: ^{1}H NMR spectrum (500 MHz, CD_3CN) of **[^{i}Pr$_2$NB(Ph)(^{Me}Im)$_2$][OTf]**.

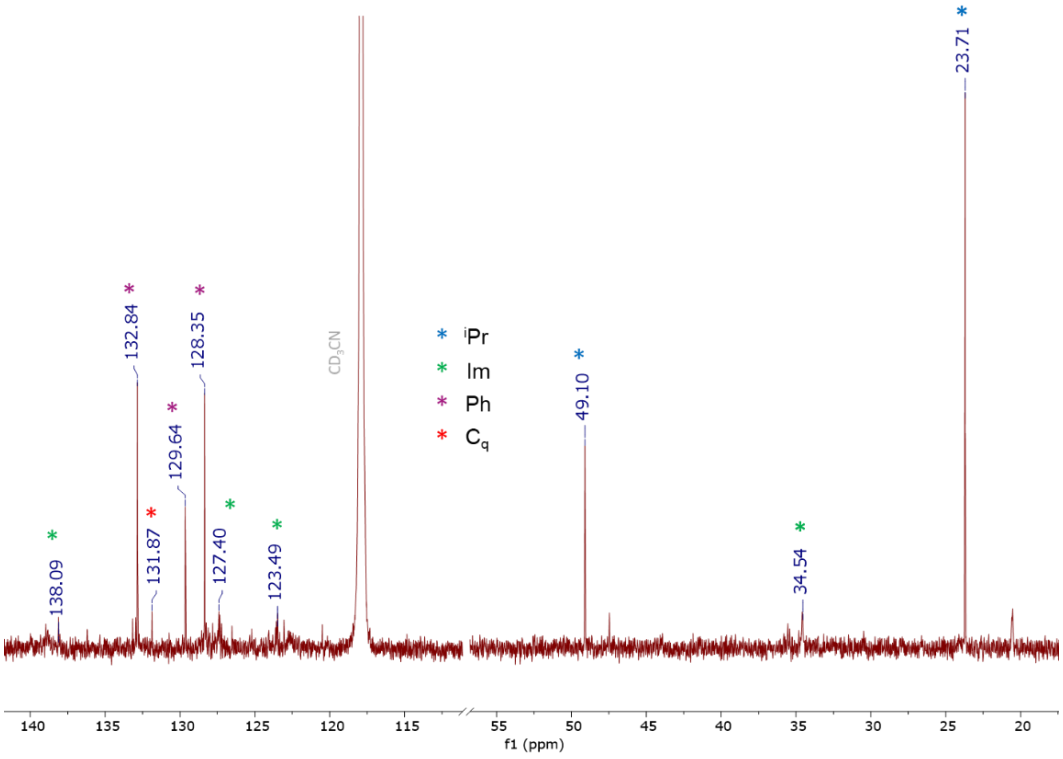

Fig 1-10: ^{13}C NMR spectrum (126 MHz, CD_3CN) of **[^{i}Pr$_2$NB(Ph)(^{Me}Im)$_2$][OTf]**.

1.4 Solvent and Anion Effects on the Formation of ^{i}Pr$_2$NB(Ph)OTf

The solution-phase identity of the product upon reacting AgOTf with $^{i}Pr_2NB(Ph)Cl$ appeared to be important for the synthesis of the imidazolium salts **[^{i}Pr$_2$NB(Ph)(^{tBu}Im)$_2$][OTf]** and **[^{i}Pr$_2$NB(Ph)(^{Me}Im)$_2$][OTf]**. Thus, several attempts to further optimize Method **C** were carried out (Scheme 1-5). First, the procedure was attempted using a different silver source, $AgPF_6$, to evaluate if aggregation or anion H-bonding effects were somehow impacting the reaction outcome. Under otherwise identical conditions outlined in Scheme 1-5, ^{1}H NMR spectra indicated that **[^{i}Pr$_2$NB(Ph)(^{Me}Im)$_2$][PF$_6$]** indeed formed, but also included unidentified impurities in the aliphatic and aromatic regions. Changing the solvent to

dichloromethane (DCM) also formed the **[^{i}Pr$_2$NB(Ph)(^{tBu}Im)$_2$][PF$_6$]** salt, but spectra indicated that P–F bond cleavage occurs, with multiple ^{31}P and ^{19}F resonances in addition to the PF_6^- septet at -144.01 ppm and doublet at -79.65 ppm, respectively. Thus, it was concluded that $AgPF_6$ is not as effective for the synthesis of **[^{i}Pr$_2$NB(Ph)(^{tBu}Im)$_2$][OTf]** and **[^{i}Pr$_2$NB(Ph)(^{Me}Im)$_2$][OTf]**.

Next, the procedure using AgOTf was attempted in DCM instead of MeCN (Scheme 1-5) for both ^{tBu}Im and ^{Me}Im. Analysis by ^{1}H, ^{11}B, and ^{19}F NMR indicates that both **[^{i}Pr$_2$NB(Ph)(^{tBu}Im)$_2$][OTf]** and **[^{i}Pr$_2$NB(Ph)(^{Me}Im)$_2$][OTf]** form, but the cleanest spectra were obtained from the original procedures carried out in MeCN. However, an interesting solvent-dependent outcome was observed when AgOTf was added to ^{i}Pr$_2$NB(Ph)Cl *prior* to the addition of imidazole. By comparing ^{1}H and ^{11}B NMR spectra during each step of the reaction, the products could be monitored based on their unique ^{11}B NMR chemical shifts. The ^{11}B NMR shift of ^{i}Pr$_2$NB(Ph)Cl appears around 36.6 ppm in both MeCN and DCM (Fig 1-11, top). After filtering off AgCl from the addition of AgOTf to ^{i}Pr$_2$NB(Ph)Cl in DCM, the ^{11}B NMR shift of a new compound appears a 30.5 ppm (Fig 1-11a, middle). Further analysis by ^{1}H and ^{13}C NMR validates the formation of the proposed triflate-coordinated product **^{i}Pr$_2$NB(Ph)OTf**. Furthermore, the ^{11}B NMR spectrum of the same reaction in MeCN shows product signals at 36.8 and 30.7 ppm, after addition of AgOTf (Fig 1-11b, middle). The signal at 36.8 ppm indicates that ^{i}Pr$_2$NB(Ph)Cl is still present in solution and the reaction has not gone to completion. Additional stirring for 2 and 24 hours did not change the product distribution by ^{11}B NMR. Nevertheless, the addition of ^{tBu}Im to both cases indicated that the reaction goes to completion,

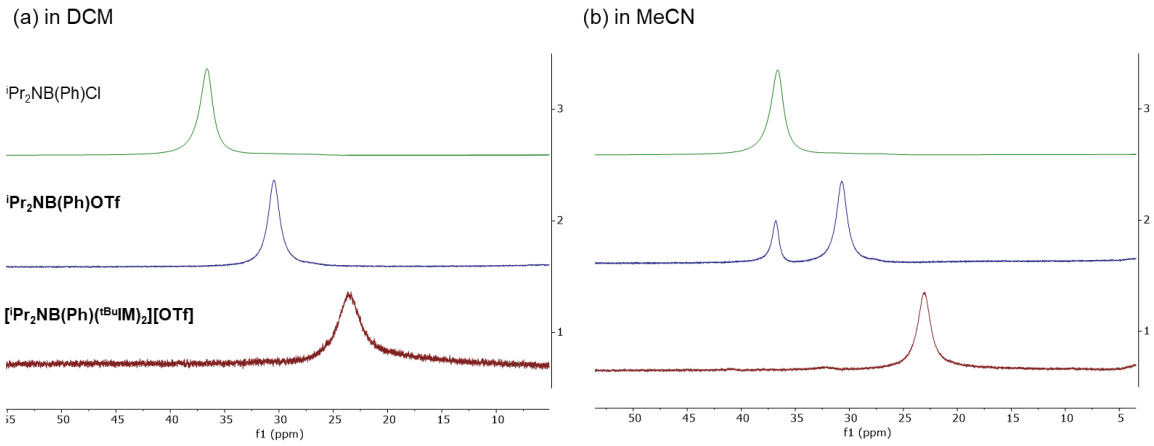

Fig 1-11: ^{11}B NMR shifts of each step in the synthesis of **[^{i}Pr$_2$NB(Ph)(^{tBu}Im)$_2$][OTf]** in (a) DCM and (b) MeCN.

successfully forming the compound **[^{i}Pr$_2$NB(Ph)(^{tBu}Im)$_2$][OTf]**. The shielding of boron in the spectra on going from starting material to product is also consistent with formation of a tetrahedral borate anion.[12] Furthermore, comparison of the ^{19}F NMR chemical shifts of **^{i}Pr$_2$NB(Ph)OTf** and **[^{i}Pr$_2$NB(Ph)(^{tBu}Im)$_2$][OTf]**, from -76.94 to -79.26 ppm, respectively, indicates the formation of a new 3-coordinate borane product.

Based on these observations, a proposed solvent-dependent reaction mechanism between AgOTf and ^{i}Pr$_2$NB(Ph)Cl is presented in Scheme 1-6. In the presence of MeCN, ^{i}Pr$_2$NB(Ph)Cl is in rapid equilibrium with solvent-bound intermediate **^{i}Pr$_2$NB(NCMe)(Ph)Cl**. Upon addition of AgOTf, a new and rapid equilibrium is proposed between ^{i}Pr$_2$NB(Ph)Cl and the unobserved intermediate **[Ag][^{i}Pr$_2$NB(OTf)(Ph)Cl]**, which can irreversibly precipitate AgCl to form the observed **^{i}Pr$_2$NB(Ph)OTf**. This is also demonstrated visually during the addition of

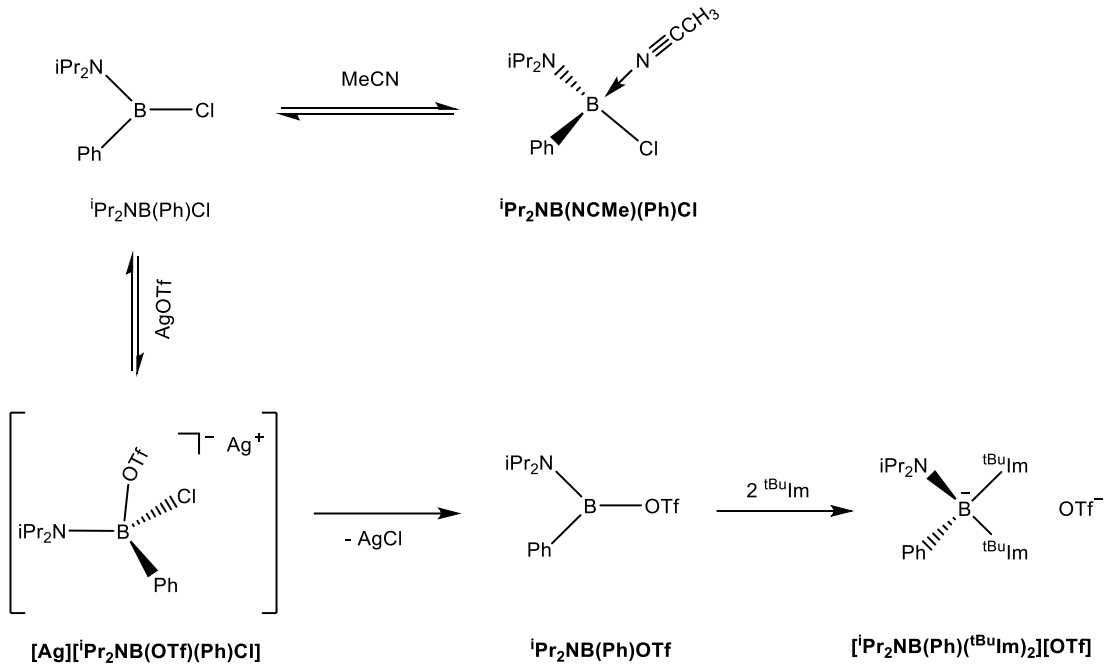

Scheme 1-6: Proposed mechanism of AgOTf and $^{i}Pr_2NB(Ph)Cl$ in MeCN.

AgOTf to $^{i}Pr_2NB(Ph)Cl$; in MeCN, a cloudy white solution forms within seconds of combining $^{i}Pr_2NB(Ph)Cl$ and AgOTf and the AgCl precipitate is filtered off to yield a pale-yellow solution. After the addition of imidazole, the pale-yellow solution turns cloudy white again, irreversibly precipitating AgCl and shifting the equilibria towards the final product. Removal of the remaining AgCl and analysis by ^{1}H and ^{11}B NMR validates the formation of **$[^{i}Pr_2NB(Ph)(^{tBu}Im)_2][OTf]$**. This phenomenon is not observed in DCM since it is a significantly weaker ligand and cannot coordinate to $^{i}Pr_2NB(Ph)Cl$ as illustrated in Scheme 1-6**.** This is also visually indicated because the reaction in DCM remains pale-yellow after removal of AgCl and subsequent addition of imidazole.

1.5 Preliminary Synthesis of the Bis(carbene)borate Ligands

A common method to synthesize N-heterocyclic carbenes is deprotonation of the parent imidazolium salts using strong bases, such as lithium bis(trimethylsilyl)amide (LiHMDS) or *n*-butyllithium (*n*-BuLi).[13] Inspired by the successful deprotonation of tris(imidazolium)borate salts, $[PhB(^{R}Im)_3][OTf]_2$ (R = ^{t}Bu, Mes), to yield tris(carbene)borate ligands,[4] initial attempts were carried out with LiHMDS. However, the ^{1}H NMR spectra obtained from several deprotonation attempts with both **[^{i}Pr$_2$NB(Ph)(^{Me}Im)$_2$][OTf]** and **[^{i}Pr$_2$NB(Ph)(^{tBu}Im)$_2$][OTf]** were inconclusive, generating an intractable mixture of products.

Preliminary attempts with *n*-BuLi appear more promising. Scheme 1-7 depicts the procedure used to synthesize the anticipated bis(carbene)borate ligand **[Li][^{i}Pr$_2$NB(Ph)(^{tBu}Im)$_2$]**. The dropwise addition of 2 equivalents of *n*-BuLi at

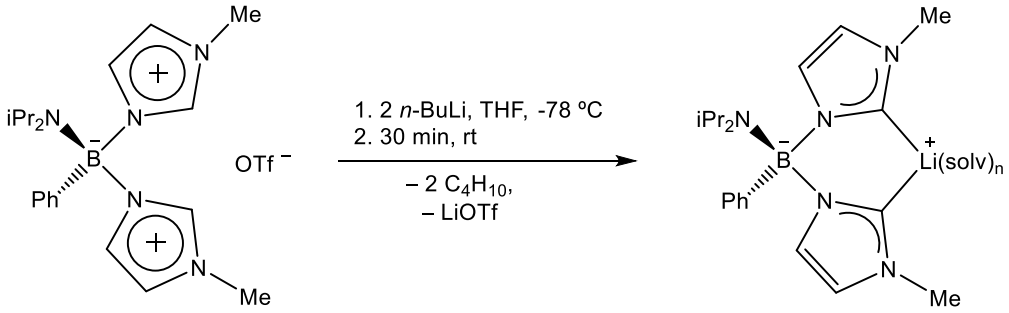

[^{i}Pr$_2$NB(Ph)(^{tBu}Im)$_2$][OTf] **[Li][^{i}Pr$_2$NB(Ph)(^{tBu}Im)$_2$]**

Scheme 1-7: Deprotonation procedure for the synthesis of the anticipated bis(carbene)borate ligand (rt = room temperature).

-78 °C to a solution of **[^{i}Pr$_2$NB(Ph)(^{tBu}Im)$_2$][OTf]** in THF followed by 30 min stirring at rt afforded the crude ^{1}H NMR spectrum at the bottom of Fig 1-12. The resultant ^{1}H NMR spectrum has several interesting features. First, the protons around

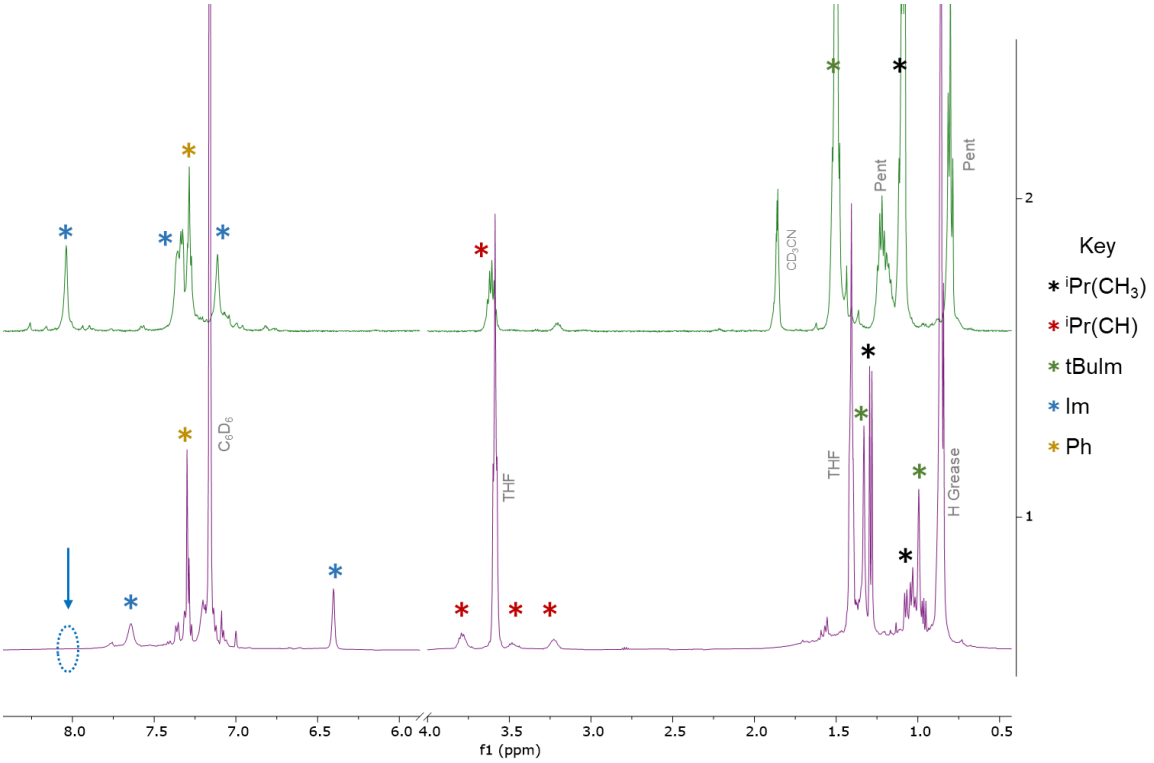

Fig 1-12: ^{1}H NMR spectra of **[^{i}Pr$_2$NB(Ph)(^{tBu}Im)$_2$][OTf]** (500 MHz, CD_3CN) before (top) and after the addition of *n*-BuLi (bottom).

8.0 ppm have disappeared after reaction with *n*-BuLi. Second, the protons from the aromatic imidazolium ring have become more shielded, most notably seen at 6.40 ppm in the bottom spectrum (blue star). Importantly, the resonance at 6.40 ppm is similar to the chemical shift of 6.81 ppm for the C-H protons of the known lithium dicarbene **[Li(Ph$_2$B(^{tBu}Im)$_2$)·Et$_2$O]**.[1] This shielding, with respect to the chemical shift of the parent imidazolium salts, supports the formation of a C=C double bond at the imidazole backbone. Third, multiple ^{i}Pr and ^{t}Bu peaks are present, suggesting the formation of dimers, solution-phase aggregates, or other unknown by-products or intermediates. Analysis by ^{1}H-^{1}H COSY indicates that there is a correlation between the multiple ^{i}Pr(CH) protons and ^{i}Pr(CH_3) protons.

The THF solvent present in the reaction solution may promote the formation of solution phase dimers, as shown in Fig 1-13 for the solid-state structures of other known lithium-dicarbene compounds reported in the literature.[1,14]

Unfortunately, no carbene signal(s) were detectable by ^{13}C NMR or ^{1}H-^{13}C HMBC and the ^{11}B NMR reveals a signal at 45.2 ppm, well within range for a 3-coordinate borane and not a 4-coordinate borate. More detailed analyses are currently under way and the exact structure of the carbene formed, if any, is currently under investigation.

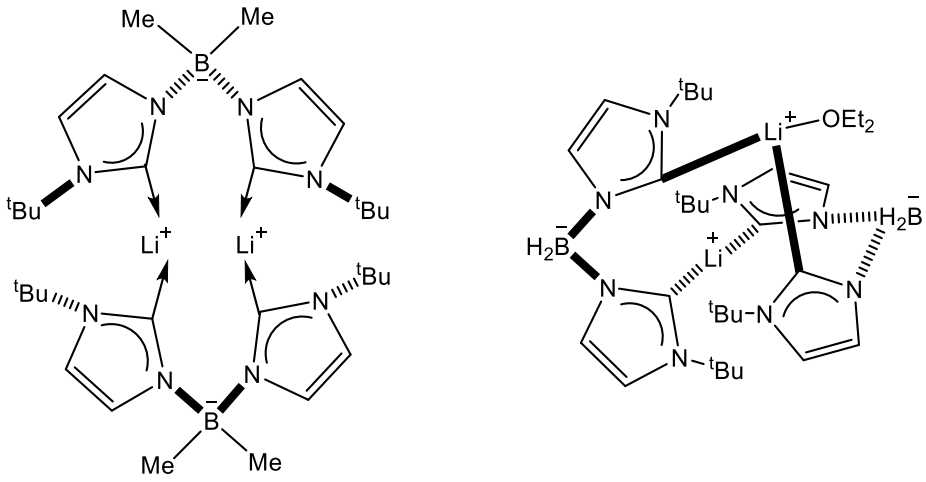

Fig 1-13: Illustration of known solid-state dimers from the literature.[1,14]

1.6 Summary and Future Work

In conclusion, two novel amine-functionalized bis(imidazolium) borate salts have been successfully synthesized and characterized; **[^{i}Pr$_2$NB(Ph)(^{Me}Im)$_2$][OTf]** and **[^{i}Pr$_2$NB(Ph)(^{tBu}Im)$_2$][OTf]**. After multiple synthetic modifications, the following conclusions can be made about the reactivity of aminoboranes with

alkylimidazoles: (1) the introduction of a better leaving group at boron, B—OTf versus B—Cl, facilitates nucleophilic substitution upon the addition of imidazole; (2) the presence of two alkylamines attached to boron is unfavorable and boron becomes a significantly weaker electrophile when two sterically bulky and electron rich amines are present; (3) the reaction outcomes using arylaminoboranes are most favorable when carried out in a coordinating solvent such as MeCN. However, more research is required to better understand the mechanism and solvent-dependency of the intermediates that lead to amine-functionalized bis(imidazolium) borate salts. Hopefully, the optimized synthetic procedure to obtain **[^{i}Pr$_2$NB(Ph)(^{Me}Im)$_2$][OTf]** and **[^{i}Pr$_2$NB(Ph)(^{tBu}Im)$_2$][OTf]** is generally applicable to other derivatives.

The preliminary deprotonation of **[^{i}Pr$_2$NB(Ph)(^{tBu}Im)$_2$][OTf]** with *n*-BuLi suggests the formation of a carbene adduct, however the ^{11}B NMR data indicates formation of a 3-coordinate borate instead of the anticipated lithium 4-coordinate borate adduct. Further research is required to better understand this deprotonation reaction. A successful transformation to generate free NHCs would make these compounds promising ligand candidates for coordination with transition metals.

If a method is developed to synthesize the aforementioned dicarbenes, future work includes the synthesis of molecular cobalt complexes by reacting the known precursor CpCo(CO)I$_2$ with lithium bis(carbene)borate salts to form a cyclopentadienylcobalt dicarbene complex and examine its reactivity with H_2 (Fig 1-14).[15] CpCo(CO)I$_2$ has been previously used to synthesize electrocatalysts with proton-responsive ligands to reduce carbon dioxide to formic acid[16] or produce

H_2.[17] Hopefully, these newly developed ligands will lead to the discovery of a new family of transition metal complexes that will behave as electrocatalysts to link renewable energy with chemical energy and ultimately create a carbon-neutral future.

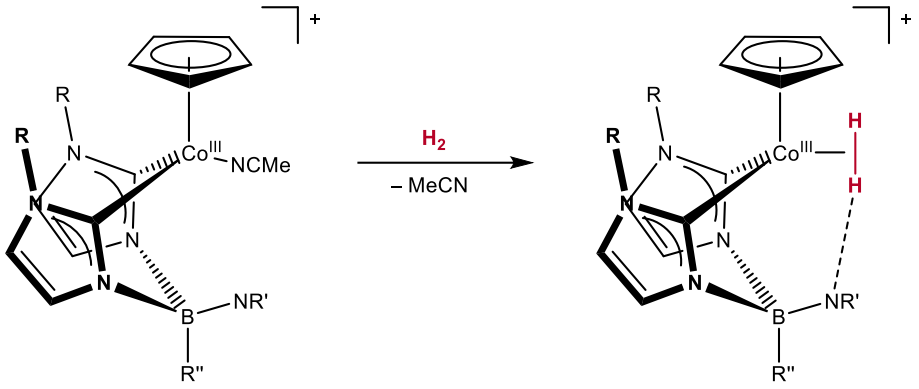

Fig 1-14: Reactivity of the anticipated cobalt complex with H_2, where R and R'/R'' are alkyl/aryl groups.

1.7 References

1. Shishkov, I.V., Rominger, F., Hofmann, P. *Organometallics*, **2009**, *28*, 3532 - 3536
2. Bailey, P.J., Lorono-Gonzales, D., McCormack, C., Millican, F., Parsons, S., Pfeifer, R., Pinho, P.P., Rudolphi, F., Perucha, A.S., *Chem Eur. J.* **2006**, *12*, 5293 – 5300
3. Haberecht, J., Krummland, A., Breher, F., Gebhardt, B., Rüegger, H., Nesper, R., Grützmacher, H. *Dalton Trans*. **2003**, 2126 - 2132
4. Cowley, R.E., Bontchev, R.P., Duesler, E.N., Smith, J.M. *Inorganic Chemistry*, **2006**, *45*, 9771 – 9779
5. Zhu, H., Vijayaraghavan, R., MacFarlane, D. R., & Forsyth, M., *Phys. Chem. Chem. Phys.* **2019**, *21*, 2691 - 2696
6. Takamuku, T., Honda, Y., Fujii, K., Kittaka, S., *Analytical Sciences*, **2008**, *24*, 1285 – 1290
7. Takamuku, T., Hoke, H., Idrissi, A., Marekha, B.A., Moreau, M., Honda, Y., Umecky, T., Shimomura, T., *Phys. Chem. Chem. Phys.* **2014**, *16*, 23627 – 12869
8. Takamuku, T., Tokuda, T., Uchida, T., Sonoda, K., Marekha, A., Idrissi, A., Takahashi, O., Horikawa, Y., Matsumura, J., Tokushima, T., Sakurai, H, Kawano, M., Sadakane, K., Iwase, H., *Phys. Chem. Chem. Phys*. **2018**, *20*, 12858 – 12869
9. Kapur, G.S., Cabrita, E.J., Berger, S., *Tetrahedron Letters*, **2000**, *41*, 7181 – 7185

10. Cohen, Y., Avram, L., Frish, L., *Angew. Chem. Int. Ed.* **2005**, *44*, 520 – 554

11. Imbery, D., Jaeschke, A., Friebolin, H., *Organic Magnetic Resonance*, **1970**, *2*, 271 – 281

12. Major, C.J., Bamford, K.L., Qu, Z.W., Stephan, D.W., *Chem. Commun.* **2019**, *55*, 5155 – 5158

13. Bullock, R.M., Catalysis Without Precious Metals, **2010**, 1st ed. Wiley-VCH

14. Nieto, I., Bontchev, R.P., Smith, J.M., *Eur. J. Inorg. Chem.* **2008**, *15*, 2476 – 2480

15. King, R.B., *Inorg. Chem.* **1966**, *5*, 82 – 87

16. Roy, S., Sharma, B., Pécaut, J., Simon, P., Fontecave, M., Tran, P.D., Derat, E., Artero, V., *J. Am. Chem. Soc.* **2017**, *139*, 3685 – 3696

17. Waldie, K.M., Kim, S.K., Ingram, A.J., Waymouth, R.M., *Eur. J. Inorg. Chem.* **2017**, 2755 – 2761

Experimental Section

1.1 General Comments

All reactions, except for the synthesis of 1-*tert*-butylimidazole (^{tBu}Im),[1] were performed either in an argon-filled glovebox or using Schlenk techniques under nitrogen. Solvents were dried over alumina using a solvent purification system and stored over activated 3 Å molecular sieves prior to use.[2] Diisopropylamine ($^{i}Pr_2NH$) was dried over NaOH and distilled under nitrogen.[3] Triethylamine (TEA) was dried with calcium hydride and distilled under nitrogen. NaI was vacuum-dried at 100 °C overnight and stored in a glove box. Celite and 1.5 µm glass fiber filters were dried overnight in an oven at 140 °C and stored in a glove box. 1-*tert*-butylimidazole and 1-methylimidazole were degassed via three freeze-pump-thaw cycles and stored over activated 3 Å molecular sieves in a glovebox. The compound $(^{i}Pr_2N)_2BCl$ was synthesized using a modified literature procedure.[4] All other reagents were purchased and used as received.

NMR spectra were recorded on Bruker Ascend^{TM} 500 MHz spectrometers at 25 °C. The ^{1}H and ^{13}C NMR chemical shifts were referenced to the residual solvent proton signals in deuterated solvent and recorded in parts per million.[6] Signal multiplicities are displayed as s, d, t, m, sept, and br for singlets, doublets, triplets, multiplets, septets, and broad, respectively. Deuterated solvents ($CDCl_3$, CD_3CN, C_6D_6, DMSO-d_6, CD_2Cl_2) were degassed via the freeze-pump thaw cycles and stored in a glovebox.

Despite multiple elemental analysis attempts on independently prepared batches of **[(^{i}Pr$_2$N)(Ph)B(^{tBu}Im)$_2$][OTf]**, results were consistently low in carbon with consistent and accurate H/N percentages. This discrepancy is attributed to the incomplete combustion of OTf^- anions.[7]

1.2 Synthetic Procedures

Modified synthesis of $^{i}Pr_2NB(Ph)Cl$ [4]

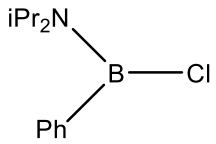

In a 100 mL Schlenk flask, an equimolar mixture of $PhBCl_2$ (2.00 g, 0.013 mol) and $^{i}Pr_2NH$ (1.28 g, 0.013 mol) was added to a solution of toluene (30 mL) and stirred. Triethylamine (1.28 g, 0.013 mol), was added at -78 °C dropwise over 5 min and the mixture was stirred overnight under N_2. The mixture was filtered through Celite and the filter pad was washed with toluene (3 x 5 mL). Drying under high vacuum provided the pure compound as a yellow-brown oil (2.52 g, 89%).

^{1}H NMR (500 MHz, $CDCl_3$): δ = 7.42 (m, 2H, Ph), 7.33 (m, 3H, Ph), 3.96 (m, 1H, CH), 3.59 (br m, 1H, CH), 1.50 (d, J = 7.0 Hz, 6H, CH_3), 1.13 (d, ^{3}J = 6.8 Hz, 6H, CH_3)

^{11}B{^{1}H} NMR (160 MHz, $CDCl_3$): δ = 36.55

Synthesis and solution-phase characterization of $^{i}Pr_2NB(Ph)OTf$

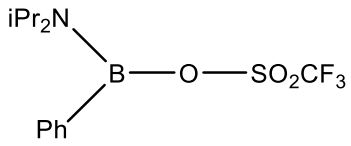

A solution of $^{i}Pr_2NB(Ph)Cl$, (34.30 mg, 0.153 mmol) in CD_2Cl_2 (0.5 mL) was added to a solution of AgOTf (39.41 mg, 0.153 mmol) in CD_2Cl_2 (0.5 mL) and immediately a white precipitate formed. The mixture was stirred overnight and filtered using glass fiber to yield a light-yellow solution, which was characterized by NMR.

^{1}H NMR (500 MHz, CD_2Cl_2): δ = 7.47 (m, 2H, Ph), 7.41 (m, 3H, Ph), 3.62 (sept, ^{3}J = 6.8 Hz, 1H, CH), 3.41 (sept, ^{3}J = 7.0 Hz, 1H, CH), 1.37 (d, ^{3}J = 7.1 Hz, 6H, CH_3), 1.08 (d, ^{3}J = 6.8 Hz, 6H, CH_3)

$^{11}B\{^{1}H\}$ NMR (160 MHz, CD_2Cl_2): δ = 30.51 ; (CD_3CN): δ = 37.06, 30.99

$^{19}F\{^{1}H\}$ NMR (471 MHz, CD_2Cl_2): δ = -76.94

$^{13}C\{^{1}H\}$ NMR (126 MHz, CD_2Cl_2): δ = 132.17 (2 CH, Ph), 131.60 (C_q, Ph), 129.84 (CH, Ph), 128.23 (2 CH, Ph), 50.47 (CH, ^{i}Pr), 45.07 (CH, ^{i}Pr), 23.72 (2 CH_3, ^{i}Pr), 21.71 (2 CH_3, ^{i}Pr)

Synthesis of [(^{i}Pr$_2$N)(Ph)B(^{tBu}Im)$_2$][OTf]

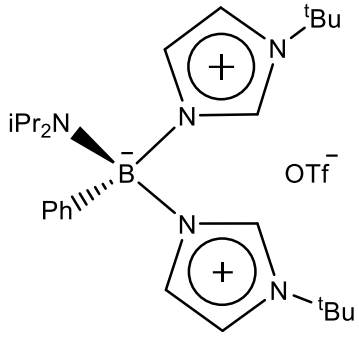

NMR Scale:

In a 20 mL vial, a solution of AgOTf (15.5 mg, 0.0605 mmol) in CD_3CN (0.35 mL) was added to a solution of $^{i}Pr_2NB(Ph)Cl$ (13.5 mg, 0.0605 mmol) in CD_3CN (0.35 mL) and immediately a white precipitate (AgCl) formed. The mixture was stirred for 20 min and filtered using glass fiber to yield a light-yellow solution, to which ^{tBu}Im (15.0 mg, 0.121 mmol) was added and stirred for 5 mins. The solution was transferred to a J. Young tube for NMR spectroscopic characterization.

Preparative Scale:

In a 20 mL vial, a solution of AgOTf (119.0 mg, 0.4633 mmol) in MeCN (3 mL) was added to a solution of $^{i}Pr_2NB(Ph)Cl$ (103.6 mg, 0.4633 mmol) in MeCN (3 mL) and immediately a white precipitate (AgCl) formed. The mixture was stirred for 20 min and filtered using glass fiber paper to yield a light-yellow solution, to which ^{tBu}Im (114.9 mg, 0.9266 mmol) was added. The solution was stirred for 20 min, filtered again, and dried under high vacuum to yield a sticky yellow precipitate. Trituration with diethyl ether (1 x 3 mL) and pentane (3 x 5 mL), followed by drying under high vacuum yielded an off-white powder (124 mg, 46%).

Anal. calcd (%) for $BN_5C_{27}H_{43}SF_3O_3$: C 55.38, H 7.40, N 11.96; found: C 54.08, H 7.36, N 11.69

^{1}H NMR (500 MHz, CD_3CN): δ = 8.09 (s, 2H, Im), 7.41 (s, 2H, Im), 7.36 (m, 2H, Ph), 7.31 (m, 3H, Ph), 7.16 (s, 2H, Im), 3.53 (sept, ^3J = 6.7 Hz, 2H, ^{i}Pr(CH)), 1.58 (s, 18H, ^{tBu}Im), 1.11 (d, ^3J = 6.9 Hz, 12H, ^{i}Pr(CH_3))

^{11}B{^{1}H} NMR (160 MHz, CD_3CN): δ = 21.43

^{19}F{^{1}H} NMR (471 MHz, CD_3CN): δ = -79.26

^{13}C{^{1}H} NMR (126 MHz, CD_3CN): δ = 135.87 (2 CH, Im), 133.44 (2 CH, Ph), 132.24 (C_q, Ph), 129.21 (CH, Ph), 128.50 (2 CH, Ph), 127.38 (2 CH, Im), 119.45 (2 CH, Im), 58.11 (C_q, Im), 48.87 (2 CH, ^{i}Pr), 30.24 (6 CH_3, Im), 24.39 (4 CH_3, ^{i}Pr)

Synthesis of [(^{i}Pr$_2$N)(Ph)B(^{Me}Im)$_2$][OTf]

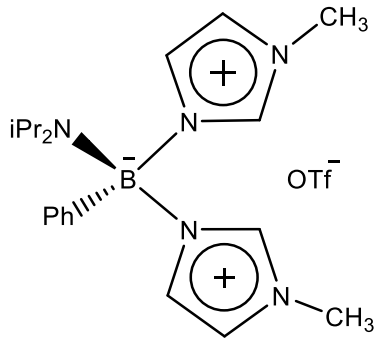

In a 20 mL vial, a solution of AgOTf (235 mg, 0.915 mmol) in CH_3CN (2 mL) was added to a solution of $^{i}Pr_2NB(Ph)Cl$ (205 mg, 0.915 mmol) in CH_3CN (2 mL) and immediately a white precipitate (AgCl) formed. The mixture was stirred for 20 min and filtered using glass fiber to yield a light-yellow solution, to which ^{Me}Im (150 mg, 1.830 mmol) was added and stirred overnight. The solution was filtered again and dried under vacuum, forming an oily yellow residue. Trituration with diethyl ether (1 X 4 mL) and pentane (4 x 5 mL), followed by drying under high vacuum yielded a pale-yellow powder (422 mg, 92%).

^{1}H NMR (500 MHz, CD_3CN): δ = 7.85 (s, 2H, Im), 7.41 (m, 2H, Ph), 7.37 (m, 3H, Ph), 7.18 (s, 2H, Im), 7.10 (s, 2H, Im), 3.74 (s, 6H, ^{Me}Im), 3.70 (m, 2H, ^{i}Pr(CH)), 1.19 (d, ^{3}J = 6.8 Hz, 12H, ^{i}Pr(CH_3))

^{11}B{^{1}H} NMR (160 MHz, CD_2Cl_2): δ = 17.34

^{19}F{^{1}H} NMR (471 MHz, CD_2Cl_2): δ = -79.01

$^{13}C\{^{1}H\}$ NMR (126 MHz, CD_3CN): δ = 138.09 (2 CH, Im), 132.84 (2 CH, Ph), 131.87 (C_q, Ph), 129.64 (CH, Ph), 128.35 (2 CH, Ph), 127.40 (2 CH, Im), 123.49 (2 CH, Im), 49.10 (2 CH, ^{i}Pr), 34.54 (2 CH_3, Im), 23.71 (4 CH_3, ^{i}Pr)

1.3 References

1. Sauerbrey, S., Majhi, P.K., Daniels, J., Schnakenburg, G., Brändle, G.M., Scherer, K., Streubel, R. *Inorg. Chem.* **2011**, *50*, 793 - 799
2. Williams, D.B.G., Lawton, M., *J. Org. Chem.* **2010**, *75*, 8351 – 8354
3. Armarego, W.L.F., Chai, C.L.L., Purification of Laboratory Chemicals, **2013**, 7th ed. Butterworth-Heinemann
4. Haberecht, J., Krummland, A., Breher, F., Gebhardt, B., Rüegger, H., Nesper, R., Grützmacher, H. *Dalton Trans*. **2003**, 2126 - 2132
5. Imbery, D., Jaeschke, A., Friebolin, H. *Organic Magnetic Resonance*, **1970**, *2*, 271 - 281
6. Fulmer, G.R., Miller, A.J.M., Sherden, N.H., Gottlieb, H.E., Nudelman, A., Stoltz, B.M., Bercaw, J.E., Goldberg, K.I., *Organometallics*, **2010**, *29*, 2176 – 2179
7. Marcó, A., Compañó, R., Rubio, R., Casals, I., *Microchim. Acta.* **2003**, *42*, 13 – 19